ScienceDirect

Mendeleev Commun., 2019, **29**, 550–552

Mendeleev
Communications

Catalytic system based on nickel(II) acetate and hypophosphorous acid for the selective hydrodeoxygenation of guaiacol

Maria A. Golubeva*[a] and Anton L. Maximov[a,b]

[a] *A. V. Topchiev Institute of Petrochemical Synthesis, Russian Academy of Sciences, 119991 Moscow, Russian Federation. Fax: +7 495 633 8520; e-mail: vinnikova@ips.ac.ru*

[b] *Department of Chemistry, M. V. Lomonosov Moscow State University, 119991 Moscow, Russian Federation*

DOI: 10.1016/j.mencom.2019.09.024

The title catalytic system exhibited high activity in the hydrogenation–hydrodeoxygenation of guaiacol (a low-molecular-weight product of lignin degradation). The conversion of guaiacol reached 97%, and the selectivity for cyclohexane was as high as 94%. Nickel phosphide phases were obtained in the reaction medium, and their presence determined the high activity of the catalytic system in the hydroconversion of guaiacol.

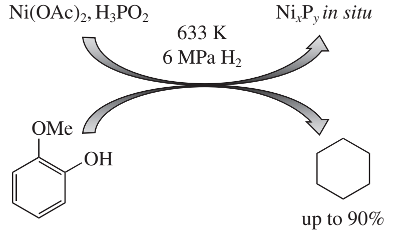

Biofuels are produced from biomass by thermochemical or biochemical conversion.[1] Biofuels have high oxygen content, as compared to that of fossil fuels. Traditional catalysts cannot be applied to novel feedstocks. For example, the activity of widely used hydrogenation (HYD) catalysts of transition metal sulfides decreases with time in low-sulfur feedstock; thus, a search for novel catalysts becomes of current interest.

Transition metal phosphides are insufficiently explored compared to transition metal sulfides. Metal-rich phosphides have metallic properties and show high chemical and thermal stability. The most active phosphide, which exhibits excellent activity in hydroprocesses, is nickel phosphide.[2,3] Nickel inorganic salts are used for the formation of nickel phosphide, nickel(II) acetate giving purer nickel phosphide compared to other salts.[4] According to thermogravimetric analysis (TGA), the main product of nickel(II) acetate decomposition in a hydrogen atmosphere is nickel, but nickel(II) oxide also forms.[5]

The synthesis of transition metal phosphides from phosphates is well known.[6–12] The temperature of reduction is 673–1273 K.[4] Lower temperatures are required if hypophosphites and hypophosphorous acid are used as a phosphorus source. Formation of phosphine occurs at 543–623 K during the disproportionation of hypophosphorous acid.[4]

$$2\,H_3PO_2 = H_3PO_4 + PH_3\uparrow$$

Nickel and nickel oxide particles react with phosphine to form nickel phosphide.[13] Generally, *ex situ* generated supported transition metal phosphides are used in hydrogenation processes. Thus, in the hydrodeoxygenation (HDO) of guaiacol, supported Ni_2P is used, which is obtained *ex situ* from phosphate[14–22] and phosphite[19,22] precursors. Anisole,[14] catechol,[19] phenol,[14–16,18,19,21] benzene,[14–18,21,22] cyclohexene[18] and cyclohexane[17,18,20,21] were obtained as main products.

We studied the HYD–HDO of guaiacol in the presence of a catalytic system based on nickel(II) acetate and hypophosphorous acid. As a result, nickel phosphide catalysts were generated *in situ* in the reaction medium. The advantages of this method are the following: phosphine, which is formed as a result of H_3PO_2 decomposition, is a poisonous gas, and the release of this gas in an autoclave *in situ* during the catalytic tests makes it possible to exclude contacts of workmen with phosphine; there is also no need to synthesize a catalyst before catalytic tests because it forms itself from precursors during the reaction. The obtained catalysts were characterized by X-ray diffraction (XRD) analysis, X-ray fluorescence (XRF) spectroscopy, and transmission electron microscopy (TEM).

Figure 1 shows the XRD patterns of the catalyst. The *in situ* generated nickel phosphide contained two phosphide phases: the most active phase of Ni_2P and slightly less active $Ni_{12}P_5$.[23] The average sizes of crystallites were estimated at 25 ± 5 nm for $Ni_{12}P_5$ and 18 ± 3 nm for Ni_2P. The patterns of $NiHPO_4 \cdot 3H_2O$ were also found. This compound may be obtained by the following reaction:[24]

$$Ni(H_2PO_2)_2 = PH_3\uparrow + NiHPO_4.$$

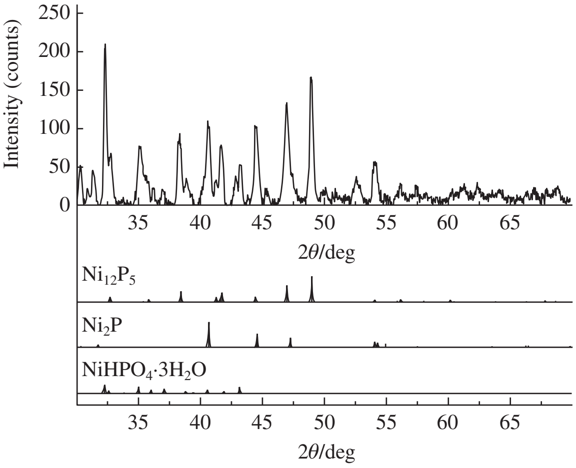

Figure 1 XRD patterns of nickel phosphide catalyst generated *in situ* during the HDO of guaiacol (633 K, 6 MPa H_2, 8 h, P : Ni = 2 : 1). Identified phases: $Ni_{12}P_5$ (PDF#22-1190), Ni_2P (PDF#03-0953), and $NiHPO_4 \cdot 3H_2O$ (PDF#39-0703).

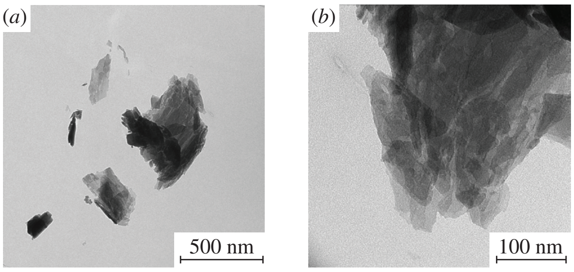

Figure 2 Microphotographs of a nickel phosphide catalyst generated *in situ* during the HDO of guaiacol (633 K, 6 MPa H_2, 8 h, P : Ni = 2 : 1).

The formation of three phases of Ni_2P, $Ni_{12}P_5$, and $NiHPO_4 \cdot 3H_2O$ from $Ni(NO_3)_2 \cdot 6H_2O$ and hypophosphorous acid H_3PO_2 as precursors was reported.[25] The formation of $Ni_{12}P_5$ phase started at about 573 K, and it was converted into Ni_2P phase at a higher temperature.[23,26]

According to the XRF analysis, the Ni : P ratio after reaction was 1.8. The initial Ni : P ratio was 1 : 2, precursors were taken in this ratio because during the decomposition of H_3PO_2, H_3PO_4 is formed along with PH_3. In addition, the amount of formed PH_3 depended on temperature.

Figure 2 shows the TEM micrographs of *in situ* generated nickel phosphide. The obtained nickel phosphide is represented by agglomerates of particles with a wide size distribution. Due to the agglomeration of unsupported particles, it is impossible to reliably calculate the average particle size using microphotographs. An electron diffraction pattern was obtained using the inverse Fourier transform of TEM images (Figure S1, Online Supplementary Materials). The lattice spacing values of 0.203 and 0.221 nm could be assigned to the (021) and (111) planes of Ni_2P or to the (330) and (202) planes of $Ni_{12}P_5$,[27] and the values of 0.211 and 0.232 nm could be assigned to the (400)[28] and (112)[27] planes of $Ni_{12}P_5$, respectively. The distribution of nickel and phosphorus in a catalyst sample (Figure S2) shows that elements are located in similar zones; thus, it can be concluded that nickel and phosphorus are contained in the same compounds.

The catalytic activity of the system based on nickel(II) acetate and hypophosphorous acid was investigated. In addition to HYD activity, nickel phosphide generated *in situ* in the catalytic system also removed oxygen from the substrates. In all experiments, cyclohexane and cyclohexene were the main products. High activity of the catalytic system in HDO can be explained by the presence of Lewis active sites in nickel phosphide catalysts.[29,30] It is assumed that Lewis acidity arises due to electron transfer from nickel to phosphorus. The HDO of guaiacol can be affected by nickel(II) hydrophosphate, which is formed as a result of decomposition of a hypophosphite precursor, as well as hypophosphorous acid, which is present in the catalytic system. All unreduced PO_x groups in the system are characterized by the presence of Brønsted active sites.[31–34] It was noted[33] that these sites are reduced at above 673 K. Among O-containing compounds, cresols, phenol, cyclohexanone, and cyclohexanol were identified. The presence of cresols as products of guaiacol HDO is associated with acidity of the catalyst. Phenol is obtained from guaiacol in an HDO process; cyclohexanol and cyclohexanone are formed *via* HDO and HYD. Cyclohexanol may also be obtained from cyclohexanone by isomerization through an enol form and the subsequent HYD of a C=C bond.

Table 1 Results of guaiacol HDO over the catalytic system based on nickel(II) acetate and hypophosphorous acid. Conditions: 5 wt% guaiacol in decaline, molar ratio P : Ni = 2 : 1, substrate : Ni = 25 : 1, 6 MPa H_2, 6 h.[a]

Temperature/K	Cyclohexane selectivity (%)	Cyclohexene selectivity (%)	HDO conversion (%)	GUA conversion (%)
553	0	6	1	17
573	15	26	19	47
593	20	46	39	59
613	35	41	60	79
633	56	17	69	94
653	77	10	85	97

[a] The conversion of guaiacol and HDO were calculated as follows: GUA conversion (%) = [(*Guaiacol*$_{in}$ – *Guaiacol*$_{out}$)/*Guaiacol*$_{in}$]100%, HDO conversion (%) = [(*Cyclohexane* + *Cyclohexene*)/*Guaiacol*$_{in}$]100%, where *Guaiacol$_{in}$* is the initial amount of guaiacol, *Guaiacol$_{out}$* is the final amount of guaiacol, and *Cyclohexane* and *Cyclohexene* are the final amounts of these products.

Table 2 Results of guaiacol HDO over the catalytic system based on nickel(II) acetate and hypophosphorous acid. Conditions: 5 wt% guaiacol in decaline, molar ratio P : Ni = 2 : 1, substrate : Ni = 25 : 1, 6 MPa H_2, 633 K.

Time/h	Cyclohexane selectivity (%)	Cyclohexene selectivity (%)	HDO conversion (%)	GUA conversion (%)
2	38	33	41	58
4	30	54	65	77
6	56	17	69	94
8	94	3	93	96

In most cases, cyclohexene was not produced in hydrodeoxygenation of guaiacol. However, earlier, cyclohexane and cyclohexene, along with phenol and benzene, were obtained as the main products of guaiacol HDO over nickel phosphide.[18] SiO_2-, ZrO_2- or activated carbon-supported Ni_2P was used as a catalyst. $Ni(NO_3)_2 \cdot 6H_2O$ and $(NH_4)HPO_4$ were used as precursors for Ni_2P synthesis. The best conversion of guaiacol (95.9%) was achieved over a Ni_2P/SiO_2 catalyst, while the selectivity for cyclohexane was 77.4%.

An increase in the process temperature from 553 to 653 K has a significant influence on product distribution (Table 1, Figure S3). At a temperature below 573 K, the formation of products did almost not occur because the decomposition of H_3PO_2 mainly starts at 573 K. A significant increase in conversion and cyclohexane selectivity occurs after 613 K. A change in the reaction time from 2 to 8 h increased selectivity for cyclohexane by a factor of 2.5 (Table 2, Figure S4). It is related to the formation of an active phase of nickel phosphide and to the contact time of a substrate with a catalyst. An increase in the hydrogen pressure from 3 to 8 MPa also raised the selectivity of cyclohexane and decreased the yield of oxygen-containing compounds (Table 3, Figure S5).

To prove that generated *in situ* nickel phosphide made the greatest contribution to the HDO of guaiacol, a series of experiments were carried out with each of the components of the catalytic system separately (Figure S6). Conversion of guaiacol was 12% and cyclohexanone was selectively obtained when nickel(II) acetate was used as a catalyst. For hypophosphorous acid used as a catalyst, conversion of guaiacol was 88% and benzene, phenol, and *o*-cresol were obtained as products. The recycling catalyst tests, including the isolation of nickel phosphide generated *in situ* in the catalytic system, were carried out (Figures S7 and S8). The results of several

Table 3 Results of guaiacol HDO over the catalytic system based on nickel(II) acetate and hypophosphorous acid. Conditions: 5 wt% guaiacol in decaline, molar ratio P : Ni = 2 : 1, substrate : Ni = 25 : 1, 633 K, 4 h.

Pressure/MPa	Cyclohexane selectivity (%)	Cyclohexene selectivity (%)	HDO conversion (%)	GUA conversion (%)
3	5	21	15	58
4	12	35	34	72
5	30	26	43	77
6	30	54	65	77
7	62	24	68	79
8	82	4	71	83

recycles showed that the catalytic activity of isolated nickel phosphide was retained, as well as its activity in the catalytic system. However, the retained activity was slightly lower than that on the first run. Thereby, it can be concluded that nickel phosphide produced in the catalytic system made the greatest contribution to the HDO of guaiacol.

In conclusion, nickel phosphide has been obtained *in situ* from nickel(II) acetate and hypophosphorous acid in the HYD–HDO reaction of guaiacol. Three nickel- and phosphorus-containing phases (Ni_2P, $Ni_{12}P_5$, and $NiHPO_4 \cdot 3H_2O$) were identified in the samples by XRD. The *in situ* generated nickel phosphide catalyst demonstrated high catalytic activity in the HYD–HDO of guaiacol (conversion of guaiacol reached 97%) and provided high cyclohexane selectivity up to 94%. The five run recycling test showed that the catalytic activity of isolated nickel phosphide was retained.

This study was supported by the Russian Foundation for Basic Research (grant no. 18-03-01186A).

Online Supplementary Materials

Supplementary data associated with this article can be found in the online version at doi: 10.1016/j.mencom.2019.09.024.

References

1 H. B. Goyal, D. Seal and R. C. Saxena, *Renewable Sustainable Energy Rev.*, 2008, **12**, 504.
2 S. T. Oyama, T. Gott, H. Zhao and Y.-K. Lee, *Catal. Today*, 2009, **143**, 94.
3 S. T. Oyama, *J. Catal.*, 2003, **216**, 343.
4 D. Liu, A. Wang, C. Liu and R. Prins, *Catal. Today*, 2017, **292**, 133.
5 J. C. De Jesus, I. Gonzalez, A. Quevedo and T. Puerta, *J. Mol. Catal. A: Chem.*, 2005, **228**, 283.
6 S. Yang, C. Liang and R. Prins, *J. Catal.*, 2006, **241**, 465.
7 G. Berhault, P. Afanasiev, H. Loboué, C. Geantet, T. Cseri, C. Pichon, C. Guillot-Deudon and A. Lafond, *Inorg. Chem.*, 2009, **48**, 2985.
8 J. Rodriguez, J.-Y. Kim, J. C. Hanson, S. J. Sawhill and M. E. Bussell, *J. Phys. Chem. B*, 2003, **107**, 6276.
9 V. M. L. Whiffen and K. J. Smith, *Energy Fuels*, 2010, **24**, 4728.
10 C. Stinner, R. Prins and T. Weber, *J. Catal.*, 2000, **191**, 438.
11 P. Clark, W. Li and S. T. Oyama, *J. Catal.*, 2001, **200**, 140.
12 R. Prins and M. E. Bussell, *Catal. Lett.*, 2012, **142**, 1413.
13 S. Yang and R. Prins, *Chem. Commun.*, 2005, 4178.
14 H. Y. Zhao, D. Li, P. Bui and S. T. Oyama, *Appl. Catal., A*, 2011, **391**, 305.
15 S.-K. Wu, P.-C. Lai, Y.-C. Lin, H.-P. Wan, H.-T. Lee and Y.-H. Chang, *ACS Sustainable Chem. Eng.*, 2013, **1**, 349.
16 S.-K. Wu, P.-C. Lai and Y.-C. Lin, *Catal. Lett.*, 2014, **144**, 878.
17 J.-S. Moon, E.-G. Kim and Y.-K. Lee, *J. Catal.*, 2014, **311**, 144.
18 J.-S. Moon, E.-G. Kim and Y.-K. Lee, *Top. Catal.*, 2015, **58**, 211.
19 S. T. Oyama, T. Onkawa, A. Takagaki, R. Kikuchi, S. Hosokai, Y. Suzuki and K. K. Bando, *Top. Catal.*, 2015, **58**, 201.
20 L. F. Feitosa, G. Berhault, D. Laurenti, T. E. Davies and V. Teixeira da Silva, *J. Catal.*, 2016, **340**, 154.
21 Y. Li, J. Fu and B. Chen, *RSC Adv.*, 2017, **7**, 15272.
22 X. Lan, E. J. M. Hensen and T. Weber, *Appl. Catal., A*, 2018, **550**, 57.
23 S. J. Sawhill, K. A. Layman, D. R. Van Wyk, M. H. Engelhard, C. Wang and M. E. Bussell, *J. Catal.*, 2005, **231**, 300.
24 Q. Guan, W. Li, M. Zhang and K. Tao, *J. Catal.*, 2009, **263**, 1.
25 B. Motos-Pérez, D. Uzio and C. Aymonier, *ChemCatChem*, 2015, **7**, 3441.
26 C. Stinner, Z. Tang, M. Haouas, T. Weber and R. Prins, *J. Catal.*, 2002, **208**, 456.
27 D. C. Costa, A. L. Soldati, G. Pecchi, J. F. Bengoa, S. G. Marchetti and V. Vetere, *Nanotechnology*, 2018, **29**, 215702.
28 Y. Pan, Y. Liu, J. Zhao, K. Yang, J. Liang, D. Liu, W. Hu, D. Liu, Y. Liu and C. Liu, *J. Mater. Chem. A*, 2015, **3**, 1656.
29 K. Li, R. Wang and J. Chen, *Energy Fuels*, 2011, **25**, 854.
30 Y.-K. Lee and S. T. Oyama, *J. Catal.*, 2006, **239**, 376.
31 I. I. Abu and K. J. Smith, *Appl. Catal., A*, 2007, **328**, 58.
32 J. A. Cecilia, A. Infantes-Molina, E. Rodríguez-Castellón, A. Jiménez-López and S. T. Oyama, *Appl. Catal., B*, 2013, **136**, 140.
33 M. E. Bussell, *React. Chem. Eng.*, 2017, **2**, 628.
34 I. V. Deliy, I. V. Shamanaev, E. Y. Gerasimov, V. P. Pakharukova, I. V. Yakovlev, O. B. Lapina, P. V. Aleksandrov and G. A. Bukhtiyarova, *Catalysts*, 2017, **7**, 298.

Received: 12th February 2019; Com. 19/5839